Structural analysis of *Phytophthora* suppressor of RNA silencing 2 (PSR2) reveals a conserved modular fold contributing to virulence

Jinqiu He[a,1], Wenwu Ye[b,1], Du Seok Choi[c,d,1], Baixing Wu[a], Yi Zhai[c,d], Baodian Guo[b], Shuyi Duan[b], Yuanchao Wang[b], Jianhua Gan[e], Wenbo Ma[c,d,2], and Jinbiao Ma[a,2]

[a]State Key Laboratory of Genetic Engineering, Ministry of Education Key Laboratory of Biodiversity Sciences and Ecological Engineering, Institute of Plant Biology, School of Life Sciences, Fudan University, 200438 Shanghai, China; [b]Department of Plant Pathology, Nanjing Agriculture University, 210095 Nanjing, China; [c]Department of Microbiology and Plant Pathology, University of California, Riverside, CA 92521; [d]Center for Plant Cell Biology, University of California, Riverside, CA 92521; and [e]State Key Laboratory of Genetic Engineering, Department of Physiology and Biophysics, School of Life Sciences, Fudan University, 200438 Shanghai, China

Edited by David C. Baulcombe, University of Cambridge, Cambridge, United Kingdom, and approved March 5, 2019 (received for review November 15, 2018)

Phytophthora **are eukaryotic pathogens that cause enormous losses in agriculture and forestry. Each *Phytophthora* species encodes hundreds of effector proteins that collectively have essential roles in manipulating host cellular processes and facilitating disease development. Here we report the crystal structure of the effector *Phytophthora* suppressor of RNA silencing 2 (PSR2). PSR2 produced by the soybean pathogen *Phytophthora sojae* (*Ps*PSR2) consists of seven tandem repeat units, including one W-Y motif and six L-W-Y motifs. Each L-W-Y motif forms a highly conserved fold consisting of five α-helices. Adjacent units are connected through stable, directional linkages between an internal loop at the C terminus of one unit and a hydrophobic pocket at the N terminus of the following unit. This unique concatenation results in an overall stick-like structure of *Ps*PSR2. Genome-wide analyses reveal 293 effectors from five *Phytophthora* species that have the *Ps*PSR2-like arrangement, that is, containing a W-Y motif as the "start" unit, various numbers of L-W-Y motifs as the "middle" units, and a degenerate L-W-Y as the "end" unit. Residues involved in the interunit interactions show significant conservation, suggesting that these effectors also use the conserved concatenation mechanism. Furthermore, functional analysis demonstrates differential contributions of individual units to the virulence activity of *Ps*PSR2. These findings suggest that the L-W-Y fold is a basic structural and functional module that may serve as a "building block" to accelerate effector evolution in *Phytophthora*.**

microbial pathogenesis | effector evolution | tandem repeats | protein diversification | *Phytophthora* disease

Phytophthora are filamentous eukaryotic pathogens that cause enormous damage to agriculture and forestry (1). Some of the most notorious species include *Phytophthora infestans*, responsible for the Great Irish Famine (2); *Phytophthora ramorum*, the causative agent of the sudden oak/larch death (3); and *Phytophthora sojae*, causing soybean stem and root rot (4). Understanding the mechanisms by which *Phytophthora* infect plants is an important step to enhance disease resistance.

Under constant challenge by parasites in the environment, plants have evolved robust innate immune systems. A central theme of plant–pathogen interactions is the activation of plant immunity on pathogen perception and the subversion of this immunity by virulence factors of the pathogens (5, 6). As hemibiotrophs, *Phytophthora* establish symbiotic associations with host plants through infection structures called haustoria. In addition to a potential role in nutrient uptake (7), haustoria are believed to be the sites in which virulence proteins are secreted (8). Some of these virulence proteins function inside the host cells and thus are termed cytoplasmic effectors (9). A majority of *Phytophthora* cytoplasmic effectors contain an N-terminal RxLR (Arg-x-Leu-Arg) motif (10, 11), and each *Phytophthora* species is predicted to encode hundreds of RxLR effectors with diverse functions (12, 13). This large effector repertoire reflects a high level of complexity in the defense/counter-defense cross-talk with hosts and warrants an in-depth analysis of their function and evolution.

Previous analysis of the functional domain of RxLR effectors revealed three motifs, named "L," "W," and "Y" after a conserved amino acid in their respective sequences (12). In particular, the W-Y (hereinafter WY) motifs, sometimes forming tandem repeats, are found in approximately 44% of *Phytophthora* RxLR effectors (14–17). Structural analyses of effectors carrying WY motif(s) uncovered a three or four α-helix bundle formed by each motif that is stabilized by a hydrophobic core (14–16, 18–21). However, the WY fold has not been demonstrated to directly contribute to the virulence activity. For example, the *P. infestans* effector PexRD54, which contains five WY repeats, relies on a C-terminal AIM motif outside the repeat region to promote infection (18, 22).

We previously identified RxLR effectors that have RNA silencing suppression activity in the host (23, 24). Among them, *Phytophthora* suppressors of RNA silencing 2 (PSR2) is produced

Significance

Effectors are essential virulence proteins. The notorious *Phytophthora* pathogens use a large arsenal of effectors to manipulate cellular processes in plant hosts. An overall understanding of effector function and the mechanisms underlying their diversification and adaptation is critical to implementing durable resistance. We analyze the protein structure of *Phytophthora* suppressor of RNA silencing 2 (PSR2), which allows the discovery of a conserved structural and functional module that tolerates sequence flexibility. Importantly, this module, often arranged as highly organized tandem repeats that are concatenated through a conserved mechanism, is present in hundreds of *Phytophthora* effectors. This study provides insight into effector evolution and offers new opportunities to combat severe *Phytophthora* diseases.

Author contributions: W.M. and J.M. conceived the project; J.H. obtained crystals of the *Ps*PSR2 protein; J.H., B.W., and J.G. collected X-ray diffraction data; B.W. and J.M. solved the crystal structure; W.Y., B.G., and Y.W. performed the bioinformatic analyses; D.C., Y.Z., and S.D. performed the functional analyses; J.M. supervised the structural analysis; W.M. supervised the bioinformatic and functional analyses; and Y.Z., B.W., J.M., W.Y., and W.M. wrote the paper

The authors declare no conflict of interest.

This article is a PNAS Direct Submission.

Data deposition: Atomic coordinates and structural factors for the crystal structure of Se-Met derivatized PsPSR2$_{59-670}$ have been deposited in the Protein Data Bank, www.wwpdb.org (PDB ID code 5GNC).

[1]J.H., W.Y., and D.S.C. contributed equally to this work.

[2]To whom correspondence may be addressed. Email: wenbo.ma@ucr.edu or majb@fudan.edu.cn.

This article contains supporting information online at www.pnas.org/lookup/suppl/doi:10.1073/pnas.1819481116/-/DCSupplemental.

Published online March 29, 2019.

by several *Phytophthora* species and is required for full virulence in *P. sojae* and *P. infestans* (23, 25, 26). Interestingly, PSR2 and its homologs contain multiple units of L-W-Y (hereinafter LWY) (27), which presumably forms a different fold than the WY motif.

Here we characterized the LWY motifs by analyzing the crystal structure of the *P. sojae* PSR2 (hereinafter *Ps*PSR2), which contains seven tandem repeats including an N-terminal WY (WY1) and six LWY units (LWY2–LWY7). WY1 forms a three α-helix fold with one hydrophobic core, similar to previous reports of other effectors (15, 18–21). However, each LWY unit comprises five α-helices with two hydrophobic pockets. Different from the previously defined L motif (12), which is 30 aa long, our structural analysis shows that the L motif spans a region of 45 aa and includes several residues (often leucine) that contribute to the formation of the additional hydrophobic core. Together with an internal loop between the W and the Y motifs from the preceding unit, this newly defined L motif is essential in connecting adjacent units in a directional manner and enables the formation of a stick-like structure of *Ps*PSR2. Importantly, 293 RxLR effectors from five *Phytophthora* species (~15% of the total number of RxLR effectors) consist of LWY motifs that are arranged using a *Ps*PSR2-like mechanism. This work highlights WY/LWY as a prevalent structural and functional module in *Phytophthora* effectors. The conserved concatenation mechanism may facilitate the diversification of *Phytophthora* effectors.

Results

Overall Structure of *Ps*PSR2. *Ps*PSR2 is a typical RxLR effector containing an N-terminal secretion signal peptide corresponding to amino acids 1–17 and an RxLR-dEER motif (amino acids 39–54) (Fig. 1*A*). The mature protein (i.e., excluding the secretion signal peptide, amino acids 18–670) was shown to promote *Phytophthora* infection when expressed in various plant hosts (23, 25, 28). We expressed the full-length mature *Ps*PSR2 protein and five truncated constructs in *Escherichia coli*. The constructs containing amino acids 59–670 ($PsPSR2_{59–670}$) and amino acids 76–670 ($PsPSR2_{76–670}$) could be crystallized, but protein diffraction was obtained only from the $PsPSR2_{59–670}$ crystals. The crystal structure of $PsPSR2_{59–670}$ was then solved using the Se-based single-wavelength anomalous diffraction method (*SI Appendix*, Fig. S1 and Table S1). We were able to obtain structural information from the amino acid 74–670 fragment of $PsPSR2_{59–670}$, which spans the entire sequence of the seven repeat units (Fig. 1*A*). The amino acid 59–73 fragment could not be modeled owing to a lack of electron density.

The overall structure of $PsPSR2_{74–670}$ consists of all α-helical folds and appears to have a stick-like shape (Fig. 1*B* and *SI Appendix*, Fig. S2*A*). There are 33 α-helices in $PsPSR2_{74–670}$. The first three, α1–α3, belong to WY1, and the rest are evenly distributed across the six LWY units (*SI Appendix*, Fig. S2 *B–H*). Superimposition demonstrates that each LWY unit forms a highly conserved helical bundle containing five α-helices (named α1′–α5′) and WY1 overlaps with the partial α3′, full α4′, and full α5′ regions of the LWY fold (*SI Appendix*, Fig. S2*I*).

LWY Is a Novel Fold Containing Two Hydrophobic Cores. The five α-helices in LWY form a stable fold centered on α3′, which has a conserved tryptophan close to the C-terminal end (Fig. 1 *C* and *D*). Similar to previously reported structures of effectors containing the WY motifs (14–16, 18–21), the tryptophan, also conserved in WY1, forms a hydrophobic interaction with a conserved tyrosine on α5′; together, these two residues stabilize a helix bundle (named HB2) comprising the C-terminal halves of α3′, α4′, and α5′ (Fig. 1 *C* and *D*).

Different from the WY motif, α3′ in the LWY motifs participates in an additional hydrophobic interaction through a conserved leucine residue (L4) on the N terminus (Fig. 1 *C* and *E*). L4 interacts with three other leucine residues, including L1 on α1′, and L2 and L3 on α2′. These leucine residues form a hydrophobic pocket and stabilize a helix bundle (named HB1) comprising α1′, α2′, and the N-terminal half of α3′ (Fig. 1 *C* and *E*). Since three of the four leucine residues that contribute to the formation of HB1 are not included in the previously described L motif (30 aa long; ref. 12), the HB1 region defines a new L motif with a length of 45 aa.

Consistent with the structural similarity, specific residues involved in the hydrophobic interactions within HB1 or HB2 are conserved in each unit despite an overall modest sequence similarity (Fig. 1*C*). Although some residues are not identical, they share similar biochemical properties and are involved in similar interactions. For example, L4 of HB1 and the tyrosine of HB2 are substituted with valine and phenylalanine, respectively, in LWY5 (Fig. 1*C*).

Directional Concatenation of Adjacent LWY Units. Intrigued by the overall structure of *Ps*PSR2, we explored the mechanism that connects adjacent units. We found a conserved loop between α4′ and α5′ in each unit except LWY7 (Fig. 1*C*). This internal loop, termed $Loop^{4-5}$, interacts with a hydrophobic pocket composed of four conserved leucine residues and several other hydrophobic residues within HB1 of the following unit (Fig. 2*A*). The pocket is hereinafter referred as the L pocket. Each $Loop^{4-5}$ has two residues inserting into the L pocket. Using the LWY2–LWY3 interaction as an example, Ile197 and Leu198 in the $Loop^{4-5}$ of LWY2 are inserted into the L pocket of LWY3 containing Leu224, Met-228, Ile240, Leu241, Thr250, Thr253, and Leu257 (Fig. 2*A*). Similarly, Leu288 and Leu289 in the $Loop^{4-5}$ of LWY3 are inserted into the L pocket of LWY4 containing Leu316, Leu319, Phe323, Leu328, Ile331, Leu332, and Leu348 (Fig. 2*A*). Similar interactions are also found in other WY/LWY pairs (*SI Appendix*, Fig. S3 *A–D*).

While residues intruding into the L pocket of the following unit are highly conserved in the $Loop^{4-5}$ from WY1 to LWY6, one of the conserved residues is substituted by a serine in LWY7 (Fig. 1*C*). In addition, there is a deletion of four amino acids in LWY7 corresponding to the region of $Loop^{4-5}$ in the other units (Fig. 1*C* and *SI Appendix*, Fig. S3*E*). These changes abolish a potential concatenation with another unit, making LWY7 an "end" unit (*SI Appendix*, Fig. S3*F*). Similarly, lacking the L motif makes WY1 a "start" unit, because it cannot connect to a preceding unit. These structural features, especially the concatenation mechanism between adjacent WY/LWY units, presumably contribute to the rigid conformation of *Ps*PSR2. There is also possible flexibility in the structure due to joints between units, which could allow for conformational changes induced by substrate binding.

The *Ps*PSR2-Like Repeat Arrangement Is Conserved in *Phytophthora* Effectors. The unique WY/LWY arrangement and the conserved concatenation in *Ps*PSR2 prompted us to investigate *Phytophthora* genomes for additional effectors with a *Ps*PSR2-like structure. We found a total of 293 RxLR effectors predicted to contain at least one LWY motif from five *Phytophthora* species (Dataset S1). The majority (84%) of these effectors also have a WY motif as the start unit following the RxLR motif. These effectors are named WY1-(LWY)n, where n is the number of LWY motifs. For example, *Ps*PSR2 would be presented as WY1-(LWY)6. The LWY motifs between the start WY1 unit and the C-terminal end unit are referred to as "middle" units (Fig. 2*B*).

Analysis of 199 WY1-(LWY)n effectors containing at least two LWY motifs (i.e., $n \geq 2$) shows that all residues participating in the hydrophobic interactions between adjacent LWY units are conserved. In particular, the residues involved in the formation of the L pocket, including the four conserved leucine residues (L1–L4), are relatively conserved in the middle and end units (Fig. 2*C*). Similarly, the two leucine residues in the $Loop^{4-5}$ are conserved in the start and middle units; however, this conservation is abolished in the end units (Fig. 2*C*). In addition, there are often deletions at and/or near the region containing these two leucine residues in the end units (Fig. 2*C* and *SI Appendix*, Figs. S4 and S5*A*). In contrast, the start units lack an intact L motif while preserving the conservation at $Loop^{4-5}$ (Fig. 2*C*). Prediction of secondary structure and surface accessibility (*SI Appendix*, Fig. S5*B*) of the start, middle, and end units also show conservation with that of *Ps*PSR2.

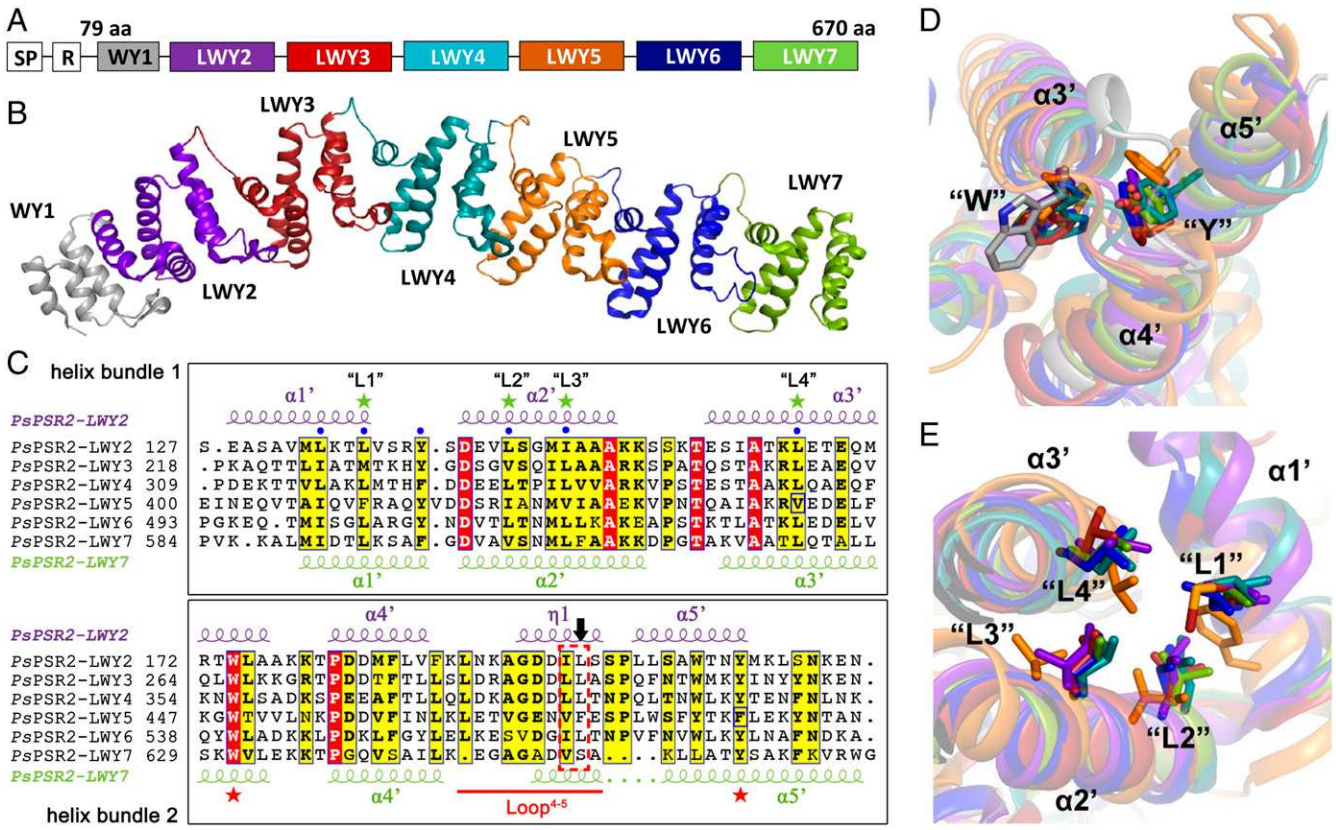

Fig. 1. *Ps*PSR2 forms a stick-like structure with two hydrophobic cores. (*A*) Schematic representation of the domain organization of *Ps*PSR2. (*B*) Overall structure of *Ps*PSR2 with cartoon-colored individual repeat units using PyMOL. (*C*) Sequence alignment of the six LWY motifs in *Ps*PSR2. The secondary structures above and below the aligned sequences are from LWY2 (purple) and LWY7 (green), respectively. The leucine residues in the L motif contributing to the hydrophobic interactions are indicated by green stars and named L1–L4. These residues and two additional hydrophobic residues in the hydrophobic pocket are indicated with blue dots. Residues from a preceding unit that are inserted into the hydrophobic pocket are boxed by red dash lines and indicated by a black arrow. The conserved tryptophan in the W motif and the tyrosine in the Y motif are indicated by red stars. The Loop$^{4\text{-}5}$ region between the W and Y motifs is highlighted. Helix bundles 1 and 2 (HB1 and HB2) are indicated with black boxes. (*D*) Close-up view of the conserved W and Y residues located in α3′ and α5′. (*E*) Close-up view of the hydrophobic contacts involving four leucine residues located in α1′, α2′, and α3′ in HB1.

Taken together, these analyses support a conserved Loop$^{4\text{-}5}$–L pocket interaction as the mechanism to form directional, stable concatenation in RxLR effectors containing LWY tandem repeats. This is consistent with the observation that the majority of LWY-containing effectors in *Phytophthora* have a WY motif as the start unit and a degenerated LWY motif as the end unit. Effectors with a single WY motif, such as AVR3a4 and AVR3a11 of *Phytophthora capsici* (15, 21), lack both the L motif and the internal loop (*SI Appendix*, Fig. S6 *A* and *B*).

LWY Represents a Unique Fold in RxLR Effectors. Structure-based searches using the DALI server (29) and a refined *Ps*PSR2 model revealed hits to helical bundles formed by RxLR effectors, especially ATR1 from *Hyaloperonospora arabidopsidis*. ATR1 is considered a WY-containing protein with a "head" region and two five-helix–containing domains (20). Comparison of the overall structures of *Ps*PSR2 and ATR1 revealed a root mean square deviation (rmsd) of 4.578 Å (main chain). The fragment spanning the two five-helix–containing domains of ATR1 align most closely with the LWY3-LWY4 region of *Ps*PSR2, with an rmsd of 2.703 (Fig. 3*A* and *SI Appendix*, Fig. S6*C*). Furthermore, the first five-helix–containing domain of ATR1 shares a structural similarity with LWY5, with a rmsd of 0.325 (*SI Appendix*, Fig. S6*D*). Importantly, the interaction between the two five-helix–containing domains in ATR1 is mediated by other interactions between an internal loop in the first unit and a hydrophobic pocket in the second unit (Fig. 3*B*). Despite the structural similarity, the residues involved in the formation of the hydrophobic pocket and their interacting residues in the loop differ from those in the LWY motifs. Nonetheless, these results indicate that ATR1 contains two tandem repeats of LWY-like units connected through a mechanism similar to the concatenation mechanism in *Ps*PSR2.

We also compared the structure of *Ps*PSR2 with that of PexRD54, which contains five WY domains. The interactions between adjacent WY pairs in PexRD54 are variable (*SI Appendix*, Fig. S6 *E–H*) and fundamentally different than the conserved directional connections found in *Ps*PSR2. This confirms that the hydrophobic pocket formed by the newly defined L motif is essential for making interunit connections in a conserved manner with a fixed orientation.

The LWY Motif Is Prevalent in *Phytophthora* Effectors. Since the LWY fold is structurally distinct from the previously characterized WY fold, we analyzed the L/W/Y-containing effectors in five *Phytophthora* species. Two additional plant pathogenic oomycetes, *H. arabidopsidis* and *Bremia lactucae*, were also included in this analysis. Each of the five *Phytophthora* genomes has a significant proportion (26–58%) of RxLR effectors containing L, W, or Y motifs (Fig. 3*C*). The L, W, or Y motifs can be predicted from 36% and 31% of total RxLR effectors from *H. arabidopsidis* and *B. lactucae*, respectively, consistent with a previous report (14).

Based on domain arrangement, we categorized the L/W/Y-containing effectors into WY1-(LWY)n ($n \geq 1$; *Ps*PSR2-like), WY1-(WY)n ($n \geq 1$; a WY1 motif followed by at least one

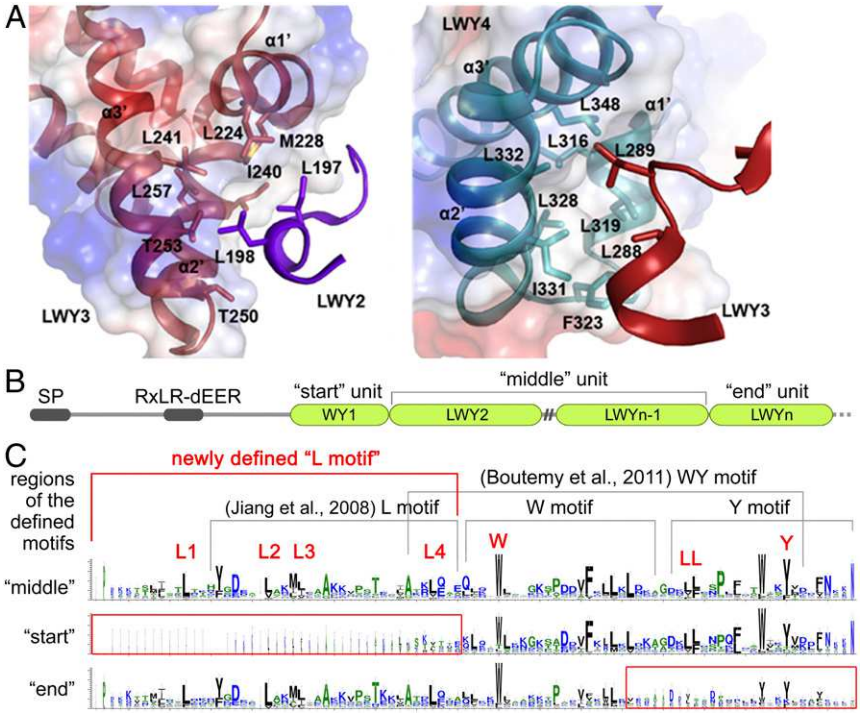

Fig. 2. Hydrophobic interactions between LWY units are conserved in WY1-(LWY)n effectors. (*A*) Detailed interactions between the Loop$^{4\text{-}5}$ of LWY2 (purple) and the hydrophobic pocket of LWY3 (burgundy), and between the Loop$^{4\text{-}5}$ of LWY3 (burgundy) and the hydrophobic pocket of LWY4 (cyan). (*B*) Schematic representation of the domain arrangement of WY1-(LWY)n type RxLR effectors. The start unit refers to an N-terminal WY1 motif; end unit, to a C-terminal LWY motif; and middle unit(s), to LWY motif(s) between the start and end units. (*C*) Weblogo presentation of sequence conservations within start, middle, and end units according to sequence alignments. The height of the stack indicates levels of conservation at that position, while the height of symbols within the stack indicates the relative frequency of each amino acid at that position. The width of the stack is proportional to the fraction of valid symbols in that position; positions with gaps have thinner stacks. The conserved leucine residues (L1–L4 and LL) involved in the hydrophobic interactions between WY and LWY or LWY and LWY, W in W motifs, and Y in Y motifs are indicated with red letters.

WY motif; PexRD54-like), WY1 (one single WY motif; AVR3a-like), or "other" (*SI Appendix*, Fig. S7 and Datasets S1–S5). A significant number of WY1-(LWY)n effectors were predicted from each genome, ranging from 28 in *P. capsici* to 84 in *P. ramorum*. Importantly, the number of WY1-(LWY)n effectors is twofold to sixfold greater than the number of WY1-(WY)n effectors in each species (Fig. 3*C*). Fourteen *H. arabidopsidis* effectors and seven *B. lactucae* effectors were predicted to have the WY1-(LWY)n arrangement. Only one WY1-(WY)n effector was predicted from *B. lactucae*, and this type of effector was not found in *H. arabidopsidis*.

The WY1-(LWY)n effectors generally have longer amino acid sequences than other RxLR effectors (Fig. 3*D*), likely due to a higher number of repeat units in these effectors. Approximately 52% of WY1-(LWY)n effectors contain two or three units, 31% contain four or five units, and 17% contain six or more units. In contrast, the majority (86%) of WY1-(WY)n effectors contain two or three units, and <4% contain six or more units (Fig. 3*E*).

We further analyzed a subset of WY1-(LWY)n and WY1-(WY)n effectors with a focus on diversification of unit sequences and unit composition in individual effectors. Clustering analysis of a similar number of WY1-(LWY)n and WY1-(WY)n effectors shows larger sequence diversity in LWY units, with the WY sequences mainly grouped into two clusters and the LWY sequences grouped into four major clusters (*SI Appendix*, Fig. S8). Importantly, the WY1-(LWY)n effectors exhibit a higher level of diversification compared with the WY1-(WY)n effectors (Fig. 4 and *SI Appendix*, Fig. S9); for example, the majority of WY1-(WY)n effectors use a start unit from the same cluster, whereas a preferred start unit cannot be identified in the WY1-(LWY)n effectors. Furthermore,

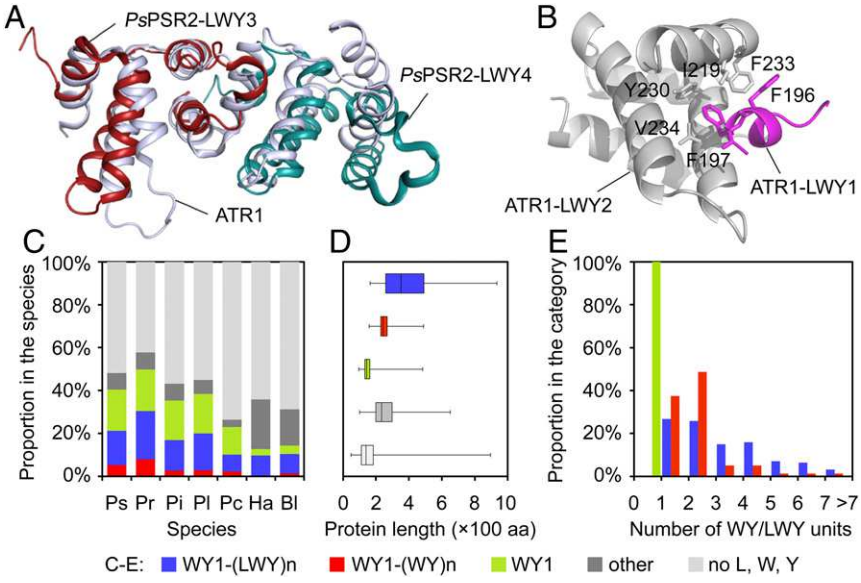

Fig. 3. LWY is a conserved structural module in oomycete effectors. (*A*) Structural similarity between the C-terminal region of the *H. arabidopsidis* effector ATR1 (gray) and the LWY3-LWY4 fragment of *Ps*PSR2. (*B*) Linkage of the two α-helix–enriched domains of ATR1 (named ATR1-LWY1 and ATR1-LWY2). Residues contributing to the hydrophobic interactions are indicated. (*C*) Distribution of RxLR effectors with indicated WY/LWY arrangement types in seven oomycete species. Bl, *B. lactucae*; Ha, *H. arabidopsidis*; Pc, *P. capsici*; Pi, *P. infestans*; Pl, *Phytophthora litchii*; Pr, *P. ramorum*; Ps, *P. sojae*. "Other" includes effectors that contain LW/Y motifs but cannot be confidently grouped into a specific arrangement type. (*D*) Boxplot showing effector length in each arrangement type. The band inside each box represents the median. Whisker ends represent the minimum and maximum values. (*E*) Distribution of effectors with different number of repeat units in each arrangement type.

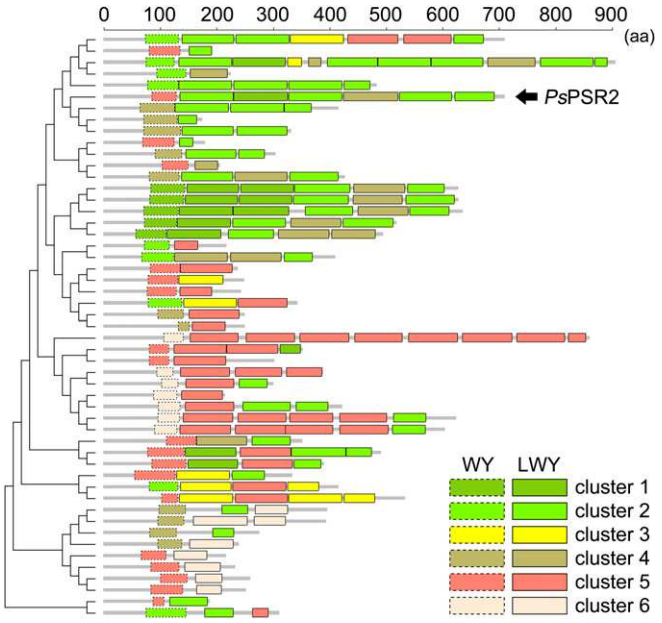

Fig. 4. Unit composition of 51 WY1-(LWY)n effectors in *P. sojae*. Amino acid sequences of individual WY/LWY units were extracted from each effector and clustered into different groups represented by different colors. Boxes with dashed lines represent predicted WY motifs, and those with solid lines represent LWY motifs. Clustering of the predicted WY and LWY regions is presented in *SI Appendix*, Fig. S8. A comparison of WY1-(LWY)n and WY1-(WY)n arrangements with a larger number of effectors is presented in *SI Appendix*, Fig. S9.

the WY1-(LWY)n effectors contain a larger variety of unit combinations, likely through recombination and duplication events, resulting in an increased complexity from a "stacking" effect. Taken together, these results suggest that the LWY motif is a prevalent fold in *Phytophthora* effectors that promotes diversification. As such, the LWY motif may play an important role in effector evolution.

We next tested whether the LWY motif functions as one module by analyzing *P. infestans* PSR2 (*Pi*PSR2), which, similar to *Ps*PSR2, has RNA silencing suppression activity and promotes *Phytophthora* infection (25). *Pi*PSR2 is the closest homolog of *Ps*PSR2. However, instead of six LWY motifs in *Ps*PSR2, *Pi*PSR2 contains seven LWY units (*SI Appendix*, Fig. S9) owing to a potential insertion of a complete middle LWY unit (*SI Appendix*, Fig. S10) in *Ps*PSR2 or a deletion of this unit in *Pi*PSR2. Interestingly, this middle unit is also found in many other WY1-(LWY)n effectors (*SI Appendix*, Fig. S9), indicating that LWY functions as a structural module to drive effector evolution.

Individual WY/LWY Units Contribute Differently to *Ps*PSR2 Activities. To evaluate the contribution of WY/LWY motif(s) to *Ps*PSR2 functions, we generated deletion mutants for each unit (*SI Appendix*, Fig. S11) and examined their activities in planta. We first determined the transgene silencing suppression activity of the *Ps*PSR2 mutants using the *Nicotiana benthamiana* transgenic plant 16c, which constitutively expresses green fluorescent protein (GFP) (30). The individual truncated gene was expressed in 16c leaves together with an external copy of the *35S-GFP* gene via *Agrobacterium* infiltration. Suppression of transgene-triggered *GFP* silencing was visualized as the recovery of green fluorescence in the infiltrated area. Similar to wild-type *Ps*PSR2, truncates with LWY3, LWY4, LWY5, or LWY7 individually deleted were able to recover *GFP* expression. In contrast, the intensity of fluorescence was compromised in the leaves expressing *Ps*PSR2$^{\Delta WY1}$, *Ps*PSR2$^{\Delta LWY2}$, or *Ps*PSR2$^{\Delta LWY6}$ (Fig. 5 and *SI Appendix*, Fig. S12*A*). This is consistent with a recent report that WY1 and LWY2 are required for *Ps*PSR2 functions by mediating its interaction with the host target double-stranded RNA-binding protein 4 (28). Similar to *Ps*PSR2$^{\Delta WY1}$ and *Ps*PSR2$^{\Delta LWY2}$, *Ps*PSR2$^{\Delta LWY6}$ also showed a reduced ability to suppress the biogenesis of small RNAs (*SI Appendix*, Fig. S12*B*). The mechanism by which LWY6 contributes to *Ps*PSR2 activity is unclear at this point.

The construct *Ps*PSR2$^{\Delta N}$, which has a deletion between the N-terminal secretion signal peptide and the WY1 unit (*SI Appendix*, Fig. S11), triggers cell death in *N. benthamiana*. Therefore, we were unable to draw a conclusion as to whether *Ps*PSR2$^{\Delta N}$ still has the ability to suppress *GFP* silencing.

To further confirm the impacts of WY1, LWY2, and LWY6 on the function of *Ps*PSR2, we examined the virulence activity of the truncated constructs. Wild-type *N. benthamiana* leaves expressing wild-type or truncated mutants of *Ps*PSR2 were inoculated with mycelium-growing agar plugs of *P. capsici* strain LT263. We observed enlarged lesions on leaves expressing wild-type *Ps*PSR2 or truncates retaining RNA silencing suppression activity, but significantly reduced virulence activities of *Ps*PSR2$^{\Delta WY1}$, *Ps*PSR2$^{\Delta LWY2}$, and *Ps*PSR2$^{\Delta LWY6}$ (*SI Appendix*, Fig. S13). Larger lesions were observed in leaves expressing *Ps*PSR2$^{\Delta N}$. Again, we refrained from drawing any conclusions, since this construct triggered cell death. Taken together, these results suggest that individual WY or LWY motifs have differential contributions to the cellular activities of *Ps*PSR2 in planta.

Discussion

The crystal structure of the *P. sojae* effector *Ps*PSR2 revealed a highly organized strand of WY/LWY repeats that are packed to form a rigid linear shape due to a conserved concatenation mechanism. We show that LWY is a basic structural module that forms a conserved five-helix fold despite limited amino acid sequence similarity. An important feature of LWY is the newly defined L motif that forms a hydrophobic pocket, which interacts with an internal loop from the preceding unit. This "joint-like" interaction establishes directional linkages that are sufficiently stable to form a highly organized linear structure and have possible flexibility to allow conformational changes on interactions with other proteins, including host targets. Without the L motif, the WY1-(WY)n effectors also lack conservation in the internal loop (*SI Appendix*, Fig. S5); therefore, these effectors must use different linkage mechanisms that are variable between

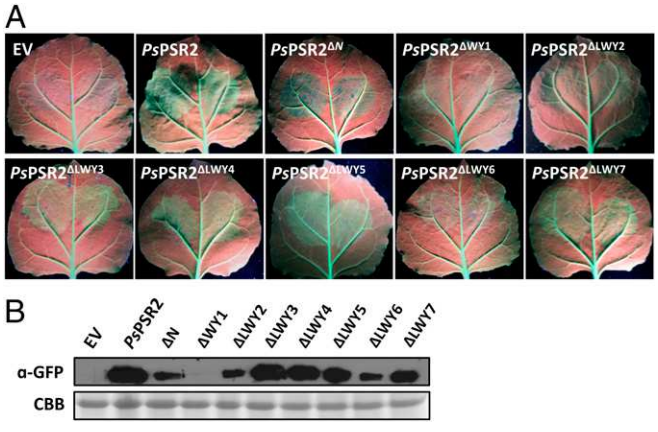

Fig. 5. Individual WY/LWY units contribute differentially to the RNA silencing suppression activity of *Ps*PSR2. Suppression of transgene silencing by wild-type and truncated *Ps*PSR2 were examined using *N. benthamiana* 16c plants. Leaves were coinfiltrated with *Agrobacterium* carrying *35S-GFP* and *Agrobacterium* harboring individual *PsPSR2* constructs (EV, empty vector; negative control). (*A*) Images of infiltrated leaves taken at 5 d after *Agrobacterium* infiltration. (*B*) GFP protein levels examined by Western blot analysis. Coomassie brilliant blue staining (CBB) served as a loading control. Experiments were repeated three times, with similar results. Note that *Ps*PSR2$^{\Delta N}$ triggers cell death in *N. benthamiana*.

different unit pairs within the same effector, such as in the case of PexRD54. Consequently, WY1-(WY)n effectors may exhibit variable overall protein shapes. In contrast, most WY1-(LWY)n effectors have well-defined start, middle, and end units and presumably also form stick-shaped molecules. Effectors containing the LWY motifs are relatively longer. Together with their extended, nonglobular architecture, these effectors have larger surface areas, which promote interactions with proteins or other molecules in the hosts.

Many tandem repeat proteins are derived from small protein domains, which act as basic structural module templates to extend protein plasticity and facilitate the evolution of novel functions. LWY motifs share limited amino acid sequence conservation, which is restricted to a small number of residues that maintain the overall structure. This sequence plasticity could contribute to differentiation of effector function through substitution of surface residues. The differential contribution of individual WY/LWY units in *Ps*PSR2 activity could be due to different surface residues of each unit. WY1-(LWY)n effectors are often chimeras of diversified LWY sequences, which may have distinct biochemical properties and/or target different host molecules. Therefore, a novel virulence function could evolve by accumulation and exchange between LWY units within and between effectors, possibly through recombination-based mechanisms. Effectors with a relatively larger number of LWY units may be able to interact with multiple host targets and facilitate infection in a "Swiss knife" manner.

Effectors are rapidly evolving molecules of the arms race with plant hosts. Tandem repeats have been proposed to promote effector family expansion, such as in the TAL effectors of bacterial pathogens (31). The WY/LWY repeats contribute to the large effector repertoire in *Phytophthora* species. The increase in effector numbers, with diversified virulence activities and a higher host targeting potential, would enhance the competitiveness of *Phytophthora* during the arms race with plant hosts.

In conclusion, this structural analysis of *Ps*PSR2 reveals a conserved functional module that may function as a basic building block of *Phytophthora* effectors to enable virulence activity and accelerate the evolution of novel functions. This discovery provides insight into fundamental mechanisms of *Phytophthora* pathogenesis and guidance to develop durable resistance.

Materials and Methods

Purified tag-free *Ps*PSR2 proteins produced in *E. coli* were screened for crystallization using a sitting-drop vapor diffusion method. The crystals of Se-Met derivatized $PsPSR2_{59–670}$ were subjected to X-ray diffraction analysis. The crystal structure was solved by the single-wavelength anomalous diffraction method and refined to acceptable R_{work}/R_{free} factors. The data diffraction and refinement statistics are summarized in *SI Appendix*, Table S1. Structural figures were generated using PyMOL (DeLano Scientific). Atomic coordinates and structure factors for the crystal structure of Se-Met–derived $PsPSR2_{59–670}$ have been deposited in the Protein Data Bank (ID code 5GNC).

Plant and microbial materials and procedures for protein purification and crystallization, structural analysis, *Phytophthora* infection, RNA silencing suppression assay, dsRNA cleavage assay, and bioinformatic analyses are described in detail in *SI Appendix* and Datasets S1–S6.

ACKNOWLEDGMENTS. This work was supported by the US Department of Agriculture's (USDA) National Institute of Food and Agriculture Awards 2014-67013-21554 and 2018-67014-28488 [jointly offered by the National Science Foundation (IOS-1758889) in the Plant Biotic Interactions Program]; USDA-AES funding CA-R-PPA-7699-H (to W.M.); and National Natural Science Foundation of China Grants 31230041 (to J.M.), 31721004 (to Y.W.), and 31772140 (to W.Y.). We thank the staff at beamline BL17U1 of the National Facility for Protein Science in Shanghai at Shanghai Synchrotron Radiation Facility for assistance with data collection.

1. Kamoun S, et al. (2015) The top 10 oomycete pathogens in molecular plant pathology. *Mol Plant Pathol* 16:413–434.
2. Zadoks JC (2008) The potato murrain on the European continent and the revolutions of 1848. *Potato Res* 51:5–45.
3. Brasier C, Webber J (2010) Plant pathology: Sudden larch death. *Nature* 466:824–825.
4. Wrather JA, Koenning SR (2006) Estimates of disease effects on soybean yields in the United States 2003 to 2005. *J Nematol* 38:173–180.
5. Jones JD, Dangl JL (2006) The plant immune system. *Nature* 444:323–329.
6. Boller T, He SY (2009) Innate immunity in plants: An arms race between pattern recognition receptors in plants and effectors in microbial pathogens. *Science* 324: 742–744.
7. Abrahamian M, Ah-Fong AM, Davis C, Andreeva K, Judelson HS (2016) Gene expression and silencing studies in *Phytophthora infestans* reveal infection-specific nutrient transporters and a role for the nitrate reductase pathway in plant pathogenesis. *PLoS Pathog* 12:e1006097.
8. Wang S, et al. (2017) Delivery of cytoplasmic and apoplastic effectors from *Phytophthora infestans* haustoria by distinct secretion pathways. *New Phytol* 216: 205–215.
9. Kamoun S (2006) A catalogue of the effector secretome of plant pathogenic oomycetes. *Annu Rev Phytopathol* 44:41–60.
10. Whisson SC, et al. (2007) A translocation signal for delivery of oomycete effector proteins into host plant cells. *Nature* 450:115–118.
11. Petre B, Kamoun S (2014) How do filamentous pathogens deliver effector proteins into plant cells? *PLoS Biol* 12:e1001801.
12. Jiang RH, Tripathy S, Govers F, Tyler BM (2008) RXLR effector reservoir in two *Phytophthora* species is dominated by a single rapidly evolving superfamily with more than 700 members. *Proc Natl Acad Sci USA* 105:4874–4879.
13. Pais M, et al. (2013) From pathogen genomes to host plant processes: The power of plant parasitic oomycetes. *Genome Biol* 14:211.
14. Win J, et al. (2012) Sequence divergent RXLR effectors share a structural fold conserved across plant pathogenic oomycete species. *PLoS Pathog* 8:e1002400.
15. Boutemy LS, et al. (2011) Structures of *Phytophthora* RXLR effector proteins: A conserved but adaptable fold underpins functional diversity. *J Biol Chem* 286: 35834–35842.
16. Franceschetti M, et al. (2017) Effectors of filamentous plant pathogens: Commonalities amid diversity. *Microbiol Mol Biol Rev* 81:e00066-16.
17. Goss EM, Press CM, Grünwald NJ (2013) Evolution of RXLR-class effectors in the oomycete plant pathogen *Phytophthora ramorum*. *PLoS One* 8:e79347.
18. Maqbool A, et al. (2016) Structural basis of host autophagy-related protein 8 (ATG8) binding by the Irish potato famine pathogen effector protein PexRD54. *J Biol Chem* 291:20270–20282.
19. Leonelli L, et al. (2011) Structural elucidation and functional characterization of the *Hyaloperonospora arabidopsidis* effector protein ATR13. *PLoS Pathog* 7:e1002428.
20. Chou S, et al. (2011) *Hyaloperonospora arabidopsidis* ATR1 effector is a repeat protein with distributed recognition surfaces. *Proc Natl Acad Sci USA* 108:13323–13328.
21. Yaeno T, et al. (2011) Phosphatidylinositol monophosphate-binding interface in the oomycete RXLR effector AVR3a is required for its stability in host cells to modulate plant immunity. *Proc Natl Acad Sci USA* 108:14682–14687.
22. Dagdas YF, et al. (2016) An effector of the Irish potato famine pathogen antagonizes a host autophagy cargo receptor. *eLife* 5:e10856.
23. Qiao Y, et al. (2013) Oomycete pathogens encode RNA silencing suppressors. *Nat Genet* 45:330–333.
24. Qiao Y, Shi J, Zhai Y, Hou Y, Ma W (2015) *Phytophthora* effector targets a novel component of small RNA pathway in plants to promote infection. *Proc Natl Acad Sci USA* 112:5850–5855.
25. Xiong Q, et al. (2014) *Phytophthora* suppressor of RNA silencing 2 is a conserved RxLR effector that promotes infection in soybean and *Arabidopsis thaliana*. *Mol Plant Microbe Interact* 27:1379–1389.
26. de Vries S, et al. (2017) Signatures of selection and host-adapted gene expression of the *Phytophthora infestans* RNA silencing suppressor PSR2. *Mol Plant Pathol* 18: 110–124.
27. Ye W, Ma W (2016) Filamentous pathogen effectors interfering with small RNA silencing in plant hosts. *Curr Opin Microbiol* 32:1–6.
28. Hou Y, et al. (2019) A *Phytophthora* effector suppresses trans-kingdom RNAi to promote disease susceptibility. *Cell Host Microbe* 25:153–165.e5.
29. Holm L, Rosenstrom P (2010) Dali server: Conservation mapping in 3D. *Nucleic Acids Res* 38:W545–W549.
30. Brigneti G, et al. (1998) Viral pathogenicity determinants are suppressors of transgene silencing in *Nicotiana benthamiana*. *EMBO J* 17:6739–6746.
31. Mesarich CH, Bowen JK, Hamiaux C, Templeton MD (2015) Repeat-containing protein effectors of plant-associated organisms. *Front Plant Sci* 6:872.